

# Pion - Nucleon Bremsstrahlung beyond the Soft-Photon approximation

A. Mariano<sup>a,b</sup>

<sup>a</sup> *Departamento de Física, Centro de Investigación y de Estudios Avanzados del IPN  
A.P. 14-740 México 07000 D.F.*

<sup>b</sup> *Departamento de Física, Facultad de Ciencias Exáctas, Universidad Nacional de La Plata  
cc.67, 1900 La Plata, Argentina*

## Abstract

A dynamical model based on effective Lagrangians is proposed to describe the bremsstrahlung reaction  $\pi N \rightarrow \pi N \gamma$  at low energies. The  $\Delta(1232)$  degrees of freedom are incorporated in a way consistent with both, electromagnetic gauge invariance and invariance under contact transformations. The model also includes the initial and final state rescattering of hadrons via a T-matrix with off the momentum-shell effects. The double differential distribution of photons is computed for three different T-matrix models and the results are compared with the soft photon approximation, and with experimental data. The aim of this analysis is to test the off-shell behaviour of the different T-matrices under consideration. Finally an alternative simpler dynamical model that incorporates the unstable character of the isobar- $\Delta(1232)$  through a complex mass, is presented. As we will see it is suitable for the study of the magnetic moment of the resonance.

PACS numbers: 25.80.Ek, 13.60.-n, 13.75.-r

# 1. INTRODUCTION

In order to extract resonant parameters of the nucleon resonances( $N^*$ ) from the  $\gamma N \rightarrow \pi N$  reaction, it is important to evaluate the background contribution to isolate the resonant peak. An important contribution to the background of this photoproduction reaction is provided by the final state rescattering (FSI) of the  $\pi N$  system [1, 2, 3, 4]. Consequently, we require the knowledge of the T-matrix that describes this rescattering process, in the off the momentum-shell regime(off-shell),i.e, we need  $T(\vec{q}', \vec{q}; z(\vec{q}))$  with  $|\vec{q}| \neq |\vec{q}'|$  where  $z$  is the total energy of the  $\pi N$  system as a function of the relative momentum  $|\vec{q}|$  of the initial state. This particular rescattering amplitude is more properly called half-off-shell T-matrix. In all cases the so called ‘realistic’ interactions are fitted to reproduce the phase shifts in elastic  $\pi N$  scattering, which only depends on the on-shell ( $|\vec{q}| = |\vec{q}'|$ ) values of the relative momenta. Thus, elastic scattering is not useful to constrain the off-shell behavior of the T-matrix because interactions working similarly in elastic scattering, may have different behaviour in the off-shell regime.

Another reaction where the  $\pi N$  off-shell T-matrix is required is  $\pi N \rightarrow \pi N \gamma$  bremsstrahlung. This process has been studied within the Soft Photon Approximation (SPA)[5]. Within this approximation the full amplitude, expressed as a power expansion in the photon energy, depends only on the electromagnetic static multipoles of  $\pi$  and  $N$  and on the T-matrix (and its derivatives) of the corresponding non-radiative process [6]. The SPA reproduces very well the experimental data on radiative  $\pi N$  scattering, in spite of some objections that have been raised recently [7] regarding the departures of the formulation of ref. [5] from the original Low’s[6] prescription. Because of the power expansion in the photon energy, the total SPA amplitude depends on the derivatives of the T-matrix, and thus on off-shell effects. Since the non-leading terms (of the power expansion) are fixed by imposing electromagnetic gauge invariance, the off-shell effects of the T-matrix cancel up mutually. Therefore, the information on the off-shell behaviour of the T-matrix can be tested by adding the contributions to the radiative  $\pi N$  scattering within the framework of an specific dynamical model.

The purpose of the present paper is to check the off-shell behaviour of three different T-matrices for  $\pi N$  rescattering in the reaction  $\pi N \rightarrow \pi N \gamma$ . We use a dynamical model to describe the  $\pi N \rightarrow \pi N \gamma$  reaction. The gauge invariant electromagnetic current is constructed explicitly, with vertices and propagators derived from the relevant hadronic and electromagnetic Lagrangians. We include also two-body meson exchange currents, and the full energy-momentum dependence of the T-matrix for the elastic  $\pi N$  scattering which exhibits its off-shell behaviour. Finally we implement this model with different T-matrices in order to compare their different off-shell dependence.

On the other hand since different T-matrices depend on many parameters (bare masses and coupling constants of the hadrons, cut-off form factor parameters, etc.), results difficult to use a dynamical model based on a T-matrix input for analyzing resonance unknown properties. For this reason we also present a simpler formalism that assumes the isobar- $\Delta$  as the main degree of freedom,

and gives it an unstable character through a complex mass. This approach will be used to study the anomalous magnetic moment of the resonance.

This paper is organized as follows. In section 2 we will construct the gauge-invariant amplitude of radiative  $\pi N$  scattering. The Lagrangians used to construct the gauge invariant current of our process, are provided also in this section. The second simpler dynamical model will be described in section 3. Finally the results and conclusions are given in section 4.

## 2. GAUGE INVARIANT BREMSSTRAHLUNG AMPLITUDE AND DYNAMICAL MODEL

In the pion-nucleon bremsstrahlung process we deal with a problem of scattering by two potentials [8]: the strong pion-nucleon and the electromagnetic interactions. The cross section for  $\pi N \rightarrow \pi N \gamma$  process reads

$$d\sigma = \int \frac{d\vec{k}}{\omega_\gamma} \int \frac{d\vec{q}_f}{\omega(\vec{q}_f)} \int \frac{d\vec{p}_f}{E(\vec{p}_f)} (2\pi)^4 \delta^4(p_i + q_i - p_f - q_f - k) \times \frac{1}{2} \sum_{\epsilon_\lambda, m_{s_f}, m_{s_i}} \left| \frac{m_N^2}{2\sqrt{2}} M_{\pi N \gamma, \pi N}(\epsilon_\lambda, k; q_f, p_f, m_{s_f}; q_i, p_i, m_{s_i}) \right|^2, \quad (1)$$

where  $q = (\omega, \vec{q})$ ,  $p = (E, \vec{p})$  and  $k = (\omega_\gamma, \vec{k})$  denote pion, nucleon and photon four-momenta, respectively;  $m_s$  is the nucleon's spin projection and  $\epsilon_\lambda$  indicates the polarization four-vector of the photon. The subindexes  $i, f$  refer to initial and final state quantities.

The Lorentz invariant amplitude<sup>1</sup>  $M_{\pi N \gamma, \pi N}$  explicitly reads

$$M_{\pi N \gamma, \pi N} = \langle \bar{u}(\vec{p}_f, m_{s_f}) | \hat{M}_{\pi N \gamma, \pi N}(\epsilon_\lambda, k; q_f, p_f; q_i, p_i) | u(\vec{p}_i, m_{s_i}) \rangle, \quad (2)$$

where  $u(\vec{p}, m_s)$  denote nucleon Dirac spinors, and the amplitude operator  $\hat{M}_{\pi N \gamma, \pi N}$  is obtained from the coupled channel Bethe-Salpeter equation for the  $\pi N \gamma$  system as follows (we consider electromagnetic interactions at the lowest order)

$$\begin{aligned} \hat{M}_{\pi N \gamma, \pi N} &= \hat{V}_{\pi N \gamma, \pi N} \\ &+ i \int \frac{dq^4}{(2\pi)^4} \left[ \hat{V}_{\pi N \gamma, \pi N}(q) \hat{G}_{\pi N}(q) \hat{M}_{\pi N, \pi N}(q) + \hat{M}_{\pi N, \pi N}(q) \hat{G}_{\pi N}(q) \hat{V}_{\pi N \gamma, \pi N}(q) \right] \\ &+ i^2 \int \frac{dq^4}{(2\pi)^4} \frac{dq'^4}{(2\pi)^4} \left[ \hat{M}_{\pi N, \pi N}(q') \hat{G}_{\pi N}(q') \hat{V}_{\pi N \gamma, \pi N}(q', q) \hat{G}_{\pi N}(q) \hat{M}_{\pi N, \pi N}(q) \right]. \end{aligned} \quad (3)$$

---

<sup>1</sup>Throughout this paper,  $M$  will denote the amplitude generated by the operator  $\hat{M}$ , i.e.,  $M = \langle \bar{u} | \hat{M} | u \rangle$ .

In terms of the above operator amplitude the T-matrix, defined as

$$\hat{T}(q_f, p_f; q_i, p_i) = \frac{1}{(2\pi)^3} \hat{M}_{\pi N, \pi N}(q_f, p_f; q_i, p_i), \quad (4)$$

satisfies the integral equation

$$\begin{aligned} \hat{T} &= \hat{U} + i \int \frac{dq^4}{(2\pi)^4} \hat{U}(q) \hat{G}(q) \hat{T}(q), \\ \hat{U} &= \frac{1}{(2\pi)^3} \hat{V}_{\pi N, \pi N}, \\ \hat{G} &= (2\pi)^3 \hat{G}_{\pi N}. \end{aligned} \quad (5)$$

In the previous equations  $\hat{V}_{ij}$  denote  $\hat{M}$ -matrix elements corresponding to the irreducible Feynman diagrams for each process, while  $\hat{G}_i$  is the product of Feynman propagators of intermediate particles.

Following the Thompson's prescription[9], we can set the above integrals in a three-dimensional form as follows (we set in the center of mass frame of the  $\pi N$  system)

$$\hat{T}(\vec{q}', \vec{q}, z) = \hat{U}(\vec{q}', \vec{q}) + \int d^3\vec{q}'' \hat{U}(\vec{q}', \vec{q}'') \hat{G}_{TH}(z, \vec{q}'') \hat{T}(\vec{q}'', \vec{q}, z), \quad (6)$$

with,

$$\hat{G}_{TH}(z, \vec{q}'') = \frac{m_N}{2\omega(\vec{q}'')E(-\vec{q}'')} \frac{\sum_{ms''} |u(-\vec{q}'', ms'')\rangle \langle \bar{u}(-\vec{q}'', ms'')|}{z - z'' + i\eta}, \quad (7)$$

where  $z'' = E(-\vec{q}'') + \omega(\vec{q}'')$ . In the above expressions  $\hat{G}_{TH}$  denotes the Thompson propagator replacing the full  $\hat{G}_{\pi N}$  Feynman propagator which, as a consequence of the three-dimensional reduction, eliminates the propagation of antiparticles and put intermediate particles on their mass-shell. The kernel function  $\hat{U}(\vec{q}', \vec{q})$  contains all the  $\pi N$ -interaction irreducible diagrams to be iterated in the T-matrix calculation, but usually only second-order contributions are kept.

The electromagnetic current  $\hat{V}_{\pi N \gamma, \pi N}$  can be broken into two pieces

$$\hat{V}_{\pi N \gamma, \pi N} \equiv \hat{V}_{\pi N \gamma, \pi N}^{(1)} + \hat{V}_{\pi N \gamma, \pi N}^{(2)}, \quad (8)$$

where the upper indices denote one- and two-body contributions, respectively which are obtained by coupling the photon to all the internal lines of  $\hat{U}$ . As is known, the operator  $\hat{V}_{\pi N \gamma, \pi N}^{(2)}$  must be added to the electromagnetic current in order to satisfy the electromagnetic gauge invariance of the total amplitude[10], while the one-body amplitude  $V_{\pi N \gamma, \pi N}^{(1)}$  vanishes for free hadrons. Both contributions to the total amplitude are illustrated in Fig. 1.

**Fig.1** One- and two-body contributions to the bremsstrahlung current amplitude.

We follow a procedure that put the bremsstrahlung amplitude manifestly gauge invariant. By replacing eqs. (4) and (5) into eq.(3), only in the one-body component of the amplitude  $M_{\pi N\gamma,\pi N}^{(1)} \equiv M_{\pi N\gamma,\pi N}(\hat{V}_{\pi N\gamma,\pi N}^{(1)})$ , we can isolate the lowest order nonzero contribution of the one-body current. After the three dimensional reduction, the total amplitude can be rewritten as

$$M_{\pi N\gamma,\pi N} \equiv \left[ \tilde{V}_{\pi N\gamma,\pi N} + \tilde{M}_{\pi N\gamma,\pi N}^{pre} + \tilde{M}_{\pi N\gamma,\pi N}^{post} + \tilde{M}_{\pi N\gamma,\pi N}^{double} \right], \quad (9)$$

with

$$\begin{aligned} \tilde{V}_{\pi N\gamma,\pi N} &= \langle \bar{u}(-\vec{q}' - \vec{k}/2, ms_f) | \hat{V}_{\pi N\gamma,\pi N}(\epsilon_\lambda, \vec{k}, \vec{q}', \vec{q}) | u(-\vec{q}, ms_i) \rangle, \\ \tilde{M}_{\pi N\gamma,\pi N}^{pre} &= \int dq''^3 \langle \bar{u}(-\vec{q}', ms_f) | \hat{T}^{(-)\dagger}(\vec{q}', \vec{q}'', z') \hat{G}_{TH}(z', \vec{q}'') \hat{V}_{\pi N\gamma,\pi N}(\epsilon_\lambda, \vec{k}, \vec{q}'', \vec{q}) | u(-\vec{q} + \vec{k}/2, ms_i) \rangle, \\ \tilde{M}_{\pi N\gamma,\pi N}^{post} &= \int dq''^3 \langle \bar{u}(-\vec{q}' - \vec{k}/2, ms_f) | \hat{V}_{\pi N\gamma,\pi N}(\epsilon_\lambda, \vec{k}, \vec{q}', \vec{q}'') \hat{G}_{TH}(z, \vec{q}'') \hat{T}(\vec{q}'', \vec{q}, z) | u(-\vec{q}, ms_i) \rangle, \\ \tilde{M}_{\pi N\gamma,\pi N}^{double} &= \int dq''^3 \int dq'''^3 \langle \bar{u}(-\vec{q}' - \vec{k}/2, ms_f) | \hat{T}^{(-)\dagger}(-\vec{q}' - \vec{k}/2, \vec{q}'', z') \\ &\quad \hat{G}_{TH}(z', \vec{q}'') \hat{V}_{\pi N\gamma,\pi N}(\epsilon_\lambda, \vec{k}, \vec{q}'', \vec{q}''') \hat{G}_{TH}(z, \vec{q}''') \hat{T}(\vec{q}''', \vec{q}, z) | u(-\vec{q}, ms_i) \rangle \end{aligned} \quad (10)$$

where the current

$$\hat{V}_{\pi N\gamma,\pi N} = i\hat{V}_{\pi N\gamma,\pi N}^{(1)}\hat{G}\hat{U} + i\hat{U}^\dagger\hat{G}\hat{V}_{\pi N\gamma,\pi N}^{(1)} + \hat{V}_{\pi N\gamma,\pi N}^{(2)} \quad (11)$$

generates a gauge invariant Born amplitude  $\tilde{V}_{\pi N\gamma,\pi N}$ , that involve all the possible ways of attaching a photon to the  $\pi N$  scattering amplitude  $U$ , and contains the full propagator  $\hat{G} \sim \hat{G}_{\pi N}$ . The operator  $\hat{T}^{(-)}(z')$ , where  $z' = z + \omega_\gamma$ , obeys eq.(6) if we change  $\eta \rightarrow -\eta$  in eq. (7).

The superscript *pre* (*post*) in Eq. (9) indicate that the photon is emitted before (after) the action of the T-matrix, while the superscript *double* refers to a double-scattering term where the photon is emitted from internal lines between two T-matrices. In the above equations the *Born*, *pre* and *double* amplitudes were evaluated in the initial center of mass frame ( $\vec{q}_f = \vec{q}' - \vec{k}/2, \vec{p}_f = -\vec{q}' - \vec{k}/2, \vec{q}_i = -\vec{p}_i = \vec{q}$ ), while the other (*post*) amplitude was evaluated in the corresponding final frame ( $\vec{q}_f = -\vec{p}_f = \vec{q}', \vec{q}_i = \vec{q} + \vec{k}/2, \vec{p}_i = -\vec{q} + \vec{k}/2$ ). The different terms in Eq. (9) are illustrated in Fig. 2a ( $\tilde{V}_{\pi N\gamma,\pi N}$ ) and in Fig. 2b (remaining terms).

**Fig.2** (a) Gauge-invariant bremsstrahlung current amplitude. (b) Post-,pre- and double-scattering amplitude contributions (se eq. (9)).

Within the SPA, the total bremsstrahlung amplitude can be split into external ( $E$ ) and internal ( $I$ ) contributions:

$$M_{\pi N\gamma,\pi N} \equiv M_{\pi N\gamma,\pi N}^E + M_{\pi N\gamma,\pi N}^I, \quad (12)$$

where we can identify

$$M_{\pi N\gamma,\pi N}^E \equiv \tilde{M}_{\pi N\gamma,\pi N}^{pre}(\hat{V}_{\pi N\gamma,\pi N} \rightarrow \hat{V}_{\pi N\gamma,\pi N}^{(1)}) + \tilde{M}_{\pi N\gamma,\pi N}^{post}(\hat{V}_{\pi N\gamma,\pi N} \rightarrow \hat{V}_{\pi N\gamma,\pi N}^{(1)}),$$

and the internal contribution  $M_{\pi N\gamma,\pi N}^I$  can be obtained “by enforcing” the gauge invariance condition

$$M_{\pi N\gamma,\pi N}(\epsilon_\lambda^\mu = k^\mu) = 0. \quad (13)$$

The SPA the  $M_{\pi N\gamma,\pi N}$  amplitude depends only on the elastic T-matrix, because derivative terms of  $\hat{T}$  cancels in the addition of internal and external contributions. Let us emphasize that any dependence on the structure of internal contributions (in particular, the dependence of off-shell effects) are of higher order in  $\omega_\gamma$  and must be included explicitly in the amplitude in a gauge invariant way.

The bremsstrahlung amplitude will be computed along the lines developed in eqs. (9-11), using a potential  $\hat{U}$  obtained from effective Lagrangians, and three specific models for the T-matrix to describe the  $\pi N$  rescattering.

The three models advocated for the T-matrix will be called OBQA, SEP and NEW, respectively. The OBQA version for the T-matrix interaction[11], is based on a model that includes  $\pi$  and  $\rho$  mesons exchange through a correlated  $2\pi$  exchange potential. The SEP model for  $\pi N$  rescattering is generated [12] by a phenomenological separable potential. Finally, the NEW model [13] is obtained from exchange of  $\pi$  and (sharp)  $\rho$  mesons. The operator  $\hat{U}$  is constructed from a Lagrangian density that includes the nucleon( $N$ ), the  $\Delta$ -isobar, and the  $\pi$ ,  $\rho$  and  $\sigma$  mesons[14]

$$\hat{\mathcal{L}}_{hadr} = \hat{\mathcal{L}}_{\pi NN} + \hat{\mathcal{L}}_{N\Delta\pi} + \hat{\mathcal{L}}_{\rho NN} + \hat{\mathcal{L}}_{\rho\pi\pi} + \hat{\mathcal{L}}_{\sigma NN} + \hat{\mathcal{L}}_{\sigma\pi\pi}, \quad (14)$$

while the electromagnetic currents are obtained from the hadronic Lagrangian density through minimal coupling of the photon. The Scattering amplitude  $U$  is depicted in Fig.3, while the amplitude  $\tilde{V}_{\pi N\gamma,\pi N}$  can be obtained by coupling the photon to all diagrams in  $U$  as shown in fig.4.

**Fig.3** Born amplitude corresponding to the  $\pi N$  potential operator  $\hat{U}$ . The first diagram denote the nucleon-pole, and the  $\Delta$ -pole corresponds to the third diagram. The fifth and sixth diagrams correspond to  $\rho$  and  $\sigma$  mesons exchange.

**Fig.4** The gauge-invariant amplitude obtained by coupling a photon to the Born terms in fig.3, together with the two-meson exchange currents (fifth, sixth and seventh graphs in each line). (a)

Contributions obtained from the N and  $\Delta$  direct-pole diagrams in fig.3; (b) Terms generated by the cross-pole diagrams in fig.3, and (c) diagrams obtained from  $\rho$  and  $\sigma$  exchange contributions in fig.3.

The good convergence properties of the scattering equations given in Eqs. (10) can be obtained by introducing hadronic form factors, which are supposed to describe the composite nature of hadrons. It is a common practice to use different parametrizations of the form factors for different T-matrices. For example, the OBQA model uses monopole and dipole forms with cutoff parameters ranging from  $\Lambda = 1200 - 1600 MeV$  [11]. In the case of the SEP interaction different form factors are introduced for each partial wave component [12], while in the NEW form factors usually advocated are of monopolar form with  $\Lambda = 1300 - 2300 MeV$  [13]. However, the introduction of form factors replacing point vertices in  $\tilde{V}_{\pi N \gamma, \pi N}$  spoils the gauge invariance of the total amplitude. Fortunately, the gauge invariance of the amplitude can be recovered by using the method of Gross and Riska [15] which, however, does not yield unique electromagnetic couplings to hadrons. Therefore, we follow the more simple prescription of using a common form factor [16, 12] of monopole type

$$f(\vec{q}') = \frac{\Lambda^2}{\Lambda^2 + \vec{q}'^2}, \quad (15)$$

where the scale  $\Lambda$  can be adjusted at a given incident energy for each T-matrix model.

### 3. DYNAMICAL MODEL II

The dynamical model described in the previous section has the advantage of describing  $\pi N$  -FSI with great detail by the inclusion of many components in the T-matrix potential. Nevertheless, these various effective contributions depend on time on certain parameters that are fitted in order to reproduce scattering phase shifts. This makes difficult to analyze (by fitting) unknown parameters of the resonances using a scattering matrix, on which we have additional parameters to be controlled. In this section we will adopt an alternative dynamical model that is simpler, and gives us a tool to study the, until this moment, unknown magnetic moment of the isobar- $\Delta(1232)$  resonance.

Taking into account that in the range of energies we will consider ( $T_{lab} \approx 300 MeV$ ) the main contribution comes from the  $\Delta$ -intermediate terms, since we are in the resonance region, we only consider the  $\Delta$ -pole contribution in the hadronic potential (third contribution in fig. 3). This reads

$$\hat{U} = \hat{\Gamma}(\pi N \rightarrow \Delta)_\nu \hat{G}^{\nu, \mu} \hat{\Gamma}(\Delta \rightarrow \pi N)_\mu, \quad (16)$$

where

$$\hat{G}^{\mu, \nu}(q) = \frac{1}{q^2 - m_\Delta^2} \hat{O}^{\mu, \nu}(q) \quad (17)$$

$$\begin{aligned}\hat{O}^{\mu,\nu}(q) &= (\not{q} + m_\Delta) \left[ -g^{\mu\nu} + \frac{1}{3}\gamma^\mu\gamma^\nu + \frac{2}{3}\frac{q^\mu q^\nu}{m_\Delta^2} - \frac{1}{3}\frac{q^\mu\gamma^\nu - q^\nu\gamma^\mu}{m_\Delta} \right] \\ &\quad - \frac{2}{3m_\Delta^2}(q^2 - m_\Delta^2) \left[ (\gamma^\mu q^\nu - \gamma^\nu q^\mu) + (\not{q} + m_\Delta)\gamma^\mu\gamma^\nu \right],\end{aligned}\quad (18)$$

is the  $\Delta$  propagator [17].

Iteration of this contribution to all orders through the T-matrix eq. (6) leads to

$$\hat{U} = \hat{\Gamma}(\pi N \rightarrow \Delta)_\nu \hat{\mathcal{G}}^{\nu,\mu} \hat{\Gamma}(\Delta \rightarrow \pi N)_\mu \quad (19)$$

where

$$\hat{\mathcal{G}}^{\mu,\nu}(q) = \frac{1}{(q^2 - m_\Delta^2)g_\alpha^\mu - \Sigma(q)_\alpha^\mu} \hat{O}^{\alpha,\nu}(q) \quad (20)$$

is a modified  $\Delta$  propagator with a self-energy

$$\Sigma(q)_\alpha^\mu = \hat{O}^{\mu\beta}(q) \int d^3p \hat{\Gamma}(\Delta \rightarrow \pi N)(p)_\beta \hat{G}(p, Z) \hat{\Gamma}(\pi N \rightarrow \Delta)(p)_\alpha.$$

In order to simplify we adopt the renormalization recipe

$$m_\Delta^2 g_\alpha^\mu + \Sigma(q)_\alpha^\mu \approx (M_\Delta^2 - iM_\Delta\Gamma)g_\alpha^\mu$$

with  $M_\Delta$  and  $\Gamma$  constants. This should be equivalent to make the replacement  $m_\Delta^2 \rightarrow M_\Delta^2 - iM_\Delta\Gamma$  in the denominator of the  $\hat{G}^{\mu,\nu}(q)$ , with which we are considering the unstable character of the  $\Delta$ . In order to get gauge invariance at the moment of coupling the photon to each line of the potential, we must make this replacement in the full propagator. Finally to calculate the bremsstrahlung amplitude within this model we must replace  $\hat{U}$  by  $\hat{U}$  in eq.(11) and keep only the born contribution in eq.(9).

The anomalous magnetic moment of the  $\Delta$ , which is not wellknown will be moved in orther to fit the region of high-energy photons since in the  $\Delta$  electromagnetic vertex

$$\hat{\Gamma}_{\nu\mu\alpha} = \hat{e}_\Delta \left[ (\gamma_\alpha g_{\nu\mu} - \frac{1}{3}\gamma_\alpha\gamma_\nu\gamma_\mu - \frac{1}{3}\gamma_\nu g_{\mu\alpha} + \frac{1}{3}\gamma_\mu g_{\nu\alpha}) - \frac{\hat{\kappa}_\Delta}{2m_\Delta} \sigma_{\alpha\beta} k^\beta g_{\nu\mu} \right], \quad (21)$$

where  $\hat{\kappa}_\Delta$  and  $\hat{e}_\Delta$  are the anomalous magnetic moment<sup>2</sup> and charge operators whose action upon the Rarita-Schwinger field give as eigenvalues the corresponding values of these properties, the  $\hat{\kappa}_\Delta$  term goes as  $\omega_\gamma$ .

---

<sup>2</sup>We restrict ourselves to the  $\Delta^{++}$  contribution, the only one for which we have experimental information on  $\kappa_\Delta$  [18].



## 4. NUMERICAL RESULTS AND CONCLUSIONS

The differential cross section  $d\sigma/d\Omega_\pi d\Omega_\gamma d\omega_\gamma$  to be compared with experimental data can be obtained from eq.(1), where the amplitude  $M_{\pi N\gamma,\pi N}$  is calculated from eqs.(9-11). The dynamical model approximation (DMA I) advocated in the present paper contains the following steps. The current operator  $\hat{V}_{\pi N\gamma,\pi N}$  is computed from the effective Lagrangian described in section 2, and the monopole form factor given in eq.(15) to have good convergence of the intermediate momentum integrals.

As is known, double scattering terms have a significant contribution in the case of *proton-proton* bremsstrahlung, mainly in the end point region of  $\omega_\gamma$  [19]. In the present work we will neglect  $\tilde{M}_{\pi N\gamma,\pi N}^{double}$  in eq.(10)), because the numerical calculation of the two three-dimensional integrals requires an enormous computation effort. Nevertheless, we keep double scattering-like contributions in *post* and *pre* amplitudes coming from current components  $i\hat{U}^\dagger\hat{G}\hat{V}_{\pi N\gamma,\pi N}^{(1)}$ , and  $i\hat{V}_{\pi N\gamma,\pi N}^{(1)}\hat{G}\hat{U}$ , respectively. In order to compare the approaches provided by the DMA I and SPA, we fix  $M_{\pi N\gamma,\pi N}$  to coincide quantitatively at low photon energies.

In addition we are going to study the sensibility of the bremsstrahlung cross section with the value of the  $\Delta$  magnetic moment. For this purpose we also evaluate the cross section through the alternative dynamical model described in section 3 (DMA II).

For illustration purposes, we will implement the DMA I approach with the OBQA, SEP and NEW T-matrices for the specific example of  $\pi^+p \rightarrow \pi^+p\gamma$ . The different coupling constants and masses needed to evaluate  $\hat{V}_{\pi N\gamma,\pi N}$  were taken from the model II of ref.[11], from [12], and from [13]. For direct pole diagrams we use bare masses and coupling constants since they get dynamically dressed in the T-matrix scattering eq.(5). In the OBQA case we replace the  $2\pi$  correlated exchange potential, by  $\pi$  and  $\rho$  sharp mass exchange terms, since they do not lead to sizable differences as shown in ref.[11]. In the SEP case we use the same coupling constants and masses, because the scattering potential is not generated from a dynamical model.

We will compare the theoretical predictions to the experimental cross sections measured by Nefkens[20](EXP), which have been reported for different kinematical configurations. In EXP the pions were detected at fixed angles  $\theta_\pi = 50.5^\circ$ ,  $\phi_\pi = 180^\circ$ , for three different energies of incident pions (269, 298 and 324 MeV), and the photons were detected at various  $\theta_\gamma, \phi_\gamma$  angles in the range of energies  $\omega_\gamma = 0 - 150$  MeV.

Our results for the cross sections in the DMA I approach, for the different ansatz of the T-matrix, are shown in Fig. 5. The SPA and experimental values are also plotted for comparison. The predictions of the DMA I approach shown in fig. 5 using the three models of the T-matrix, are compared to the results of EXP for photon angles given by  $G_{14} \equiv \theta_\gamma = 103^\circ, \phi_\gamma = 180^\circ$ . Since the parameters entering T-matrices are usually quoted to reproduce the elastic phase shifts, the cutoff parameters  $\Lambda$  were fixed in order to have good coincidence between the predictions of the

different interactions and the SPA at low  $\omega_\gamma$  values. We get (in MeV units)  $\Lambda_{OBQA} = 750, 700, 600$ ,  $\Lambda_{SEP} = 700, 600, 500$ , and  $\Lambda_{NEW} = 550, 500, 450$ , for incident pion energies  $T_{lab} = 269, 298, 324$  respectively. Observe that the value of  $\Lambda$  found in the case of the SEP interaction for  $T_{lab} = 298 MeV$  is consistent with the one previously found for pion photo-production at  $T_{lab} = 300 MeV$ [12], while the OBQA values are roughly consistent with the form factors used in ref.[11], which corresponds to a monopole form-factor with  $\Lambda \approx 800 MeV$ [16].

**Fig.5**  $\pi N\gamma$  cross section for  $T_{lab} = 269, 298$  and  $324 MeV$  and  $G_{14} \equiv \theta_\gamma = 103^\circ, \phi_\gamma = 180^\circ$  in EXP, calculated in the DMA I for the different T-matrices. We also include the SPA cross section and the measured values.

Results for the cross section within the DMA II are shown in Fig. 6 for different photon detectors,  $G_{14} \equiv \theta_\gamma = 103^\circ, \phi_\gamma = 180^\circ$ ;  $G_{11} \equiv \theta_\gamma = 160^\circ, \phi_\gamma = 180^\circ$ ; and  $G_7 \equiv \theta_\gamma = 120^\circ, \phi_\gamma = 0^\circ$ . We will fix  $M_\Delta = 1232 MeV$  and  $\Gamma = 110 MeV$  as reported in previous experimental works[21]. The coupling constant  $f_{N\Delta\pi}$ , was determined fitting the low-energy photon emission region (elastic scattering). We obtained  $f_{N\Delta\pi} = 0.24$ , which is in the range of previous works. Independently, the  $\Delta$  magnetic moment  $\kappa_\Delta$  was shifted in order to show how the high energy photon region can be fitted.

**Fig.6**  $\pi N\gamma$  cross section for  $T_{lab} = 269 MeV$  and  $G_7 \equiv \theta_\gamma = 120^\circ, \phi_\gamma = 0^\circ$ ,  $G_{11} \equiv \theta_\gamma = 160^\circ, \phi_\gamma = 0^\circ$ , and  $G_{14} \equiv \theta_\gamma = 103^\circ, \phi_\gamma = 180^\circ$  in EXP, calculated in the DMA II for two different values of  $\kappa_\Delta$ .

In almost all the cases, the predictions of the DMA I (fig.5) lies above the experimental cross section and the SPA for energies  $\omega_\gamma > 20 MeV$ . One of the reasons for this may be the use of an overall form factor to cure the gauge invariance problems. The total bremsstrahlung amplitude is built up, as can be seen from eqs. (9) and (10), by adding different components. It is not expected that the common form factor works satisfactorily by adding up these components as it does the one used to generate the individual T-matrices, which change their values from vertex to vertex. The comparison between the results of the SPA and DMA I schemes shows that the additional off-shell effects, added coherently to the lowest order contributions, may have important contributions since they do not cancel exactly with the derivate terms of the T-matrix appearing from the soft-photon expansion.

From fig.5 we can check that the SEP interaction provides the closest results to the experimental cross section with a departure starting for  $\omega_\gamma > 40 MeV$ . This indicates that the dynamical model involved in the SEP interaction gives the smallest off-shell effects. On the other hand, the strongest off-shell effects appear in the OBQA model. This conclusion agrees with a previous study[16] on observables in pion photo-production experiments.

As it was discussed in section 2, the off-shell contributions to the external and internal amplitudes within the SPA cancel each other, thus we cannot study these effects within this approximation. In addition since we get gauge invariance in the SPA by adjusting the internal amplitude, the gauge-

invariant electromagnetic currents remain hidden. In the DMA I approach, these cancellation must occur explicitly between the different components of the amplitude (the so-called born,pre,post contributions). The departure of the different T-matrices from the SPA can be used to estimate the size of unbalanced off-shell terms and provide a test of their off-shell behaviors. Also, since the electromagnetic gauge-invariant current is constructed explicitly from effective Lagrangians, we can use the radiative  $\pi N$  reaction to study the relevance of the degrees of freedom and the parameters involved in this dynamical model.

On the other hand from fig.6 we can see as this reaction within the DMA II (tree-label + complex  $M_\Delta$ ), is sensible to the changes of  $\kappa_\Delta$ . This model seems appropriated to analyze the anomalous magnetic moment of the  $\Delta$  resonance, since within the SPA the the 'enforcing' gauge invariant procedure does not fix this term, which is self-gauge invariant. In order to give a realistic value , a more carefull fitting procedure of  $M_\Delta$ ,  $\Gamma$ , and  $\kappa_\Delta$ , must be done.

## ACKNOWLEDGMENTS

The work of A. Mariano was supported in part by Conacyt (México) through the Fondo de Cátedras Patrimoniales de Excelencia Nivel II, and Conicet (Argentina). He is also grateful to G. López Castro for important discussions.

## References

- [1] S. Nozawa and T.-S.H. Lee , Nuc. Phys.,**A513**,511(1990).
- [2] T.-S.H. Lee and and B.C. Pearce, Nucl. Phys.,**A530**,532(1991).
- [3] Y. Surya and F. Gross, Phys. Rev. **C53**, 2422(1996).
- [4] T. Sato and T.-S.H. Lee, Phys. Rev. **C54**, 2660(1996).
- [5] M.K. Liou and Z.M. Ding, Phys. Rev. **C35**, 651(1987).
- [6] F.E. Low, Phys. Rev. **110**, 974(1958).
- [7] M. Welsh and H. Fearing, Phys. Rev. **C54**, 2240(1996).
- [8] M.L. Golderberger and K.M. Watson, Collision Theory, (John Wiley &. Sons, New York, 1964)
- [9] R. Thompson, Phys. Rev. **D1**, 110(1970).
- [10] K. Nakayama, *Perspectives in the Structure of Hadronic Systems* ,(M.N. Haraken et. al., Plenum Press, New York, 1994)

- [11] C. Schütz, J.W. Durso, K. Holinde, and J. Speth, Phys. Rev. **C49**, 2671(1994).
- [12] S. Nozawa, B. Blankleider and T.-S.H. Lee, Nuc. Phys., **A513**,459(1990);S. Nozawa, T.-S.H. Lee, and B. Blankleider, Phys. Rev., **C41**,213(1990).
- [13] O. Krehl, PhD Thesis, 1999, University of Bonn, unpublished.
- [14] J. Wess and B. Zumino, Phys. Rev. **163**, 1727(1967).
- [15] F. Gross and D.O. Riska, Phys. Rev. **C36**, 1928(1987).
- [16] K. Nakayama, Ch. Schutz, S. Krewald, J. Speth, and W. Pfeil,"CEBAF/INT Workshop on N\* Physics." , ed. by T. S.- Lee and R. Williams, 1996, World Scientific.
- [17] M. El Amiri, G. López Castro, and J. Pestieau, Nuc. Phys.**A543**, 673(1992).
- [18] D. Lin , M.K. Lioun and Z.M. Ding, Phys. Rev. **C44**, 1819(1991).
- [19] V. Herrmann, J. Speth and K. Nakayama, Phys. Rev. **C43**, 394(1991).
- [20] B.M.K. Nefkens et. al., Phys. Rev. **D18**, 3911(1978).
- [21] E. Pedroni et al., Nuc. Phys. **A300**, 321(1978).

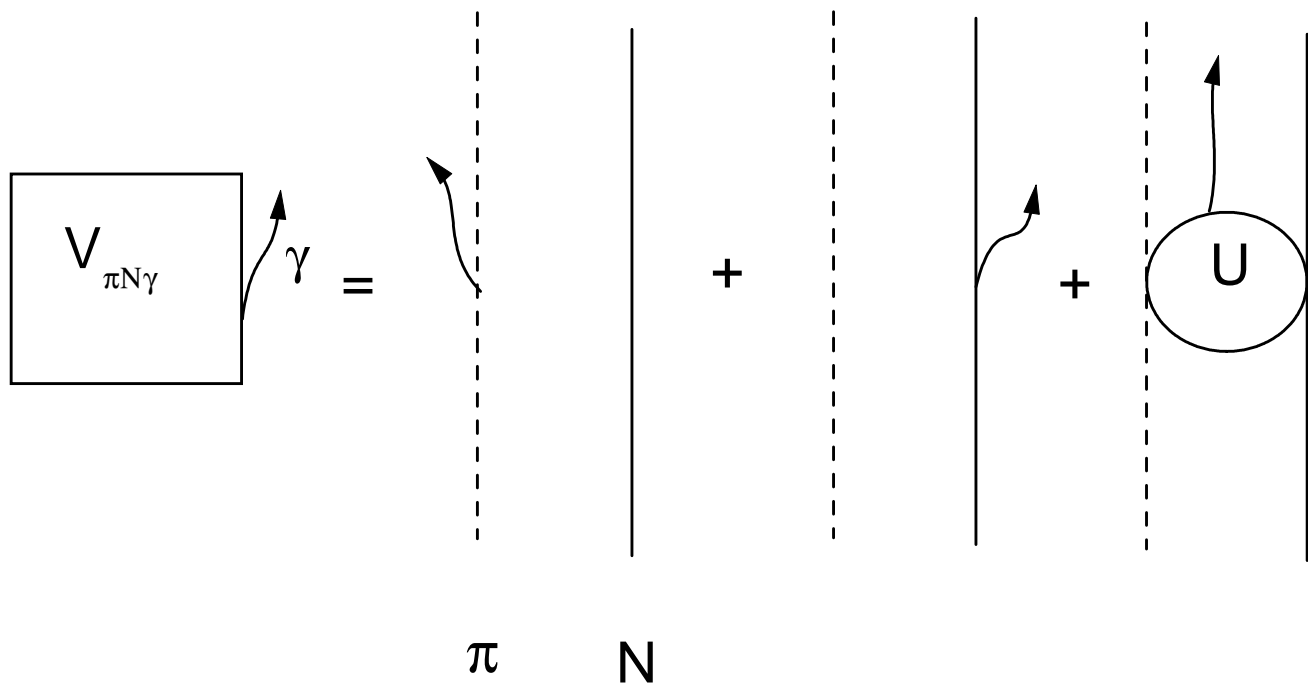
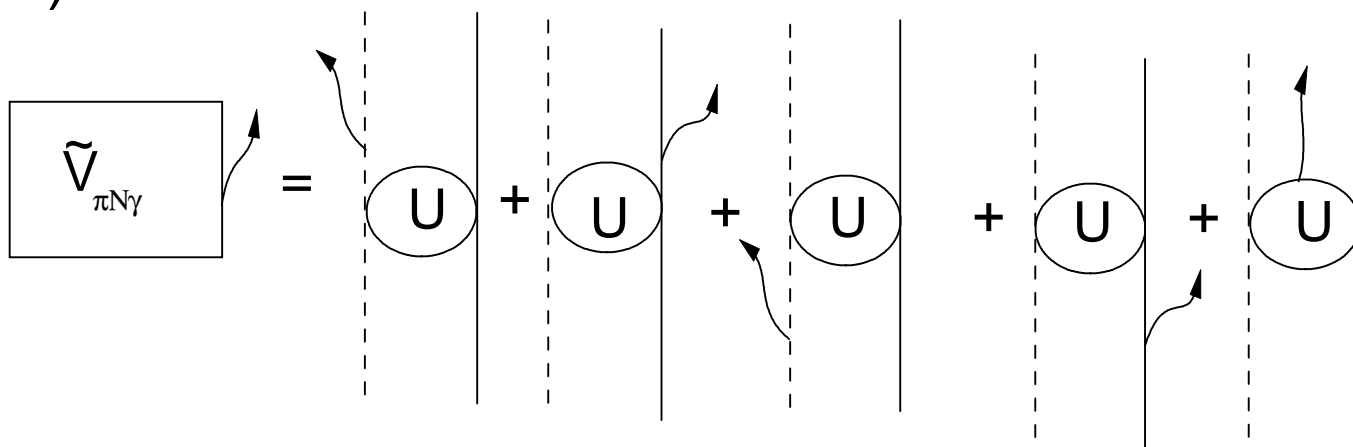


figure 1

**a)**



**b)**

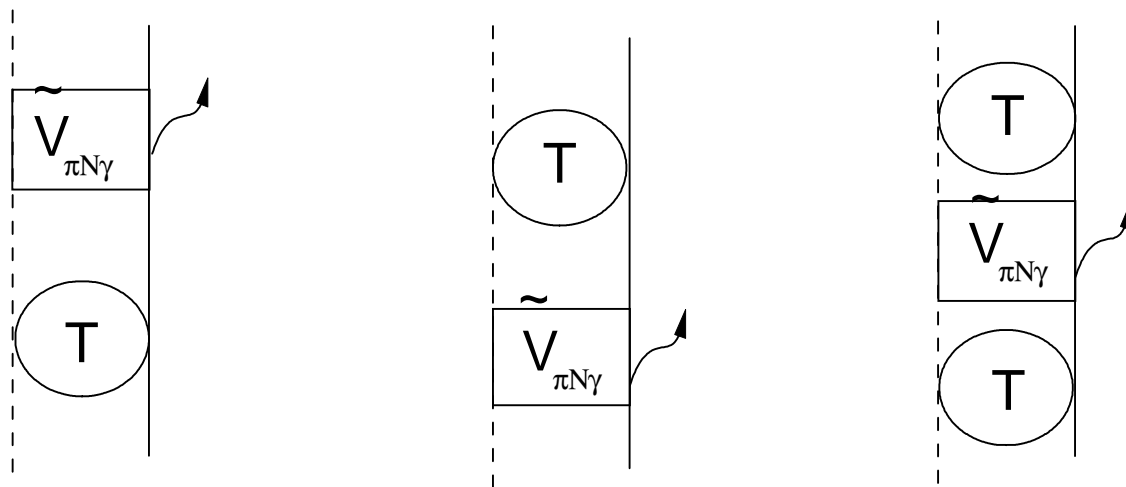


figure 2

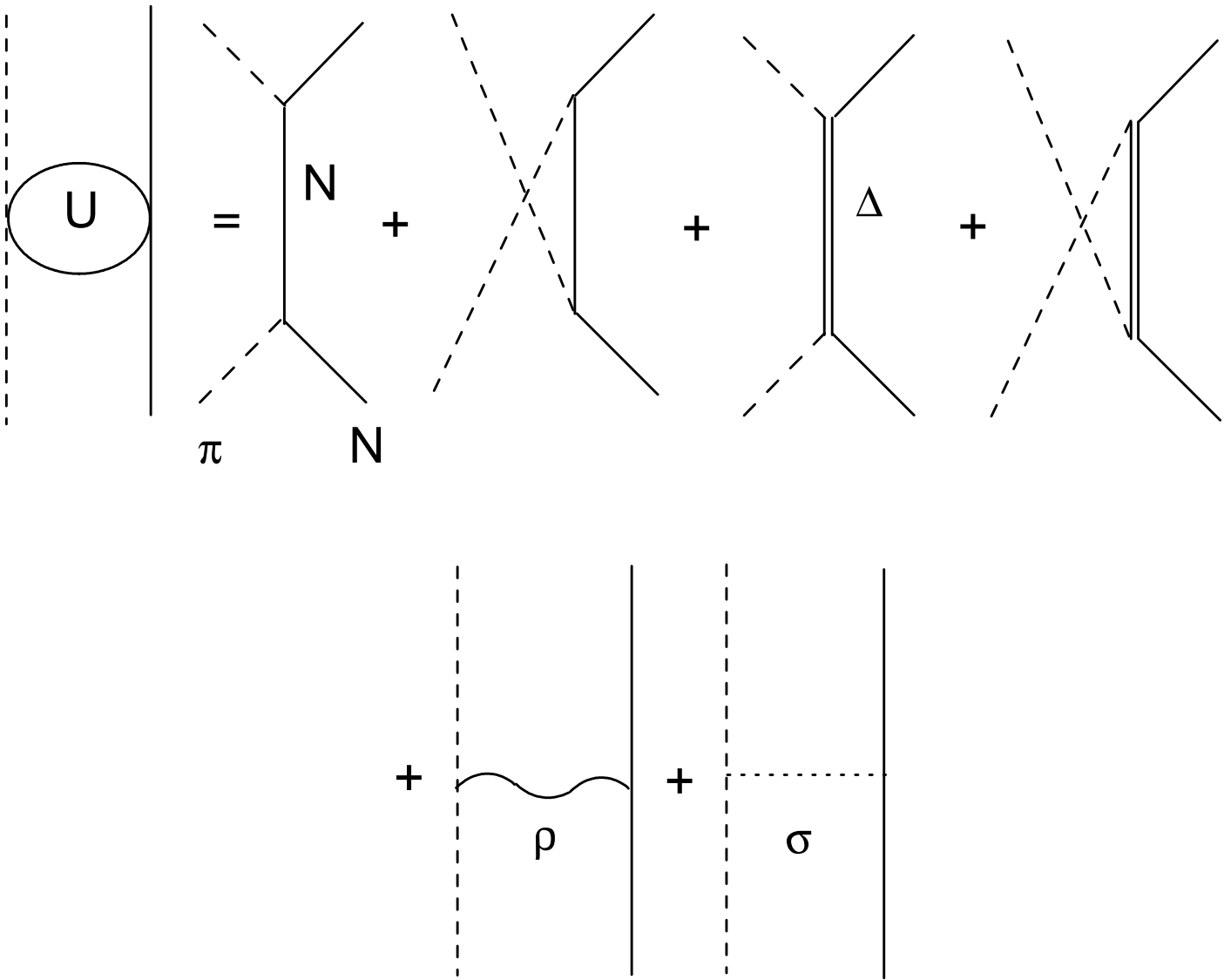


figure 3

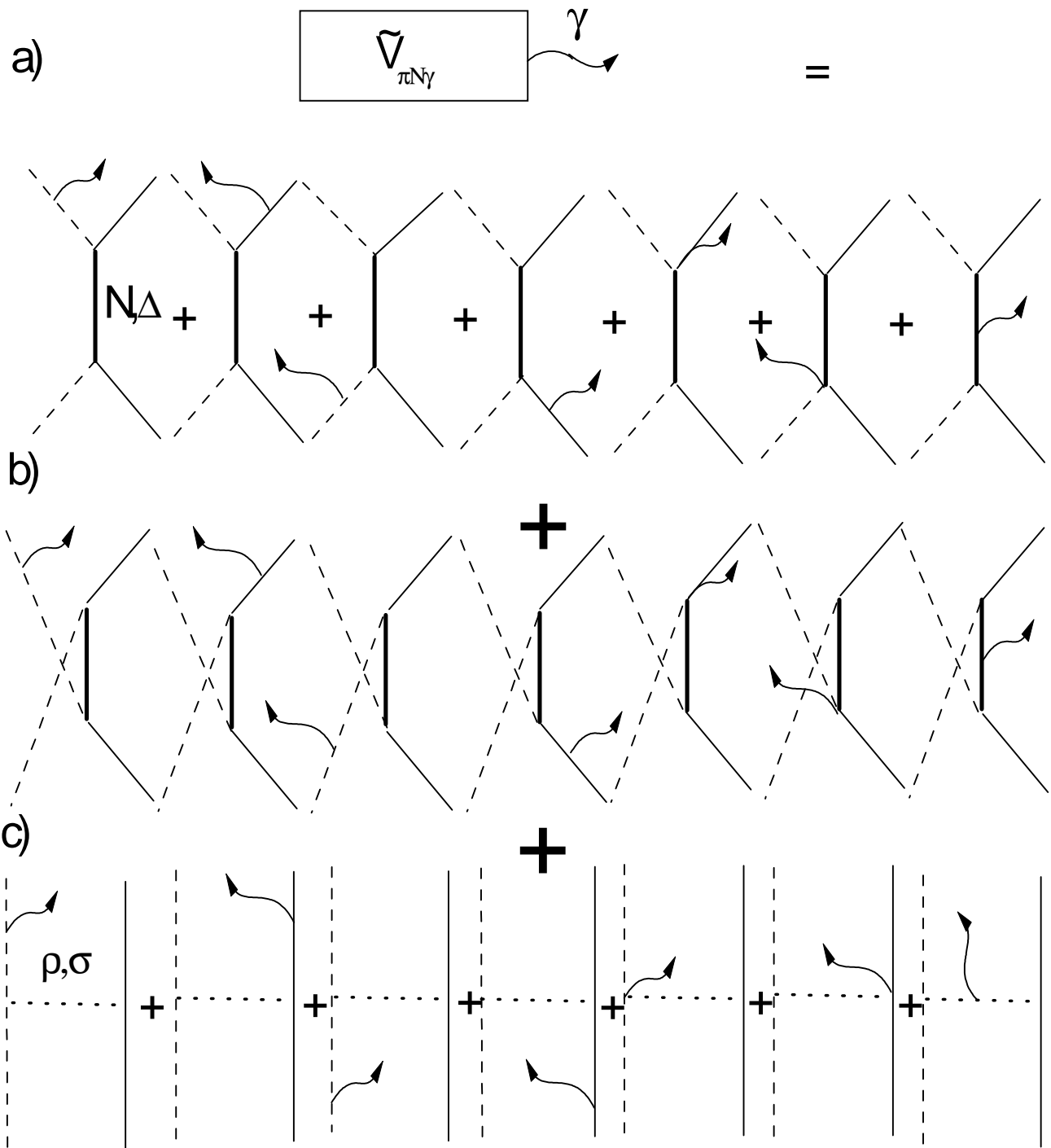


figure 4



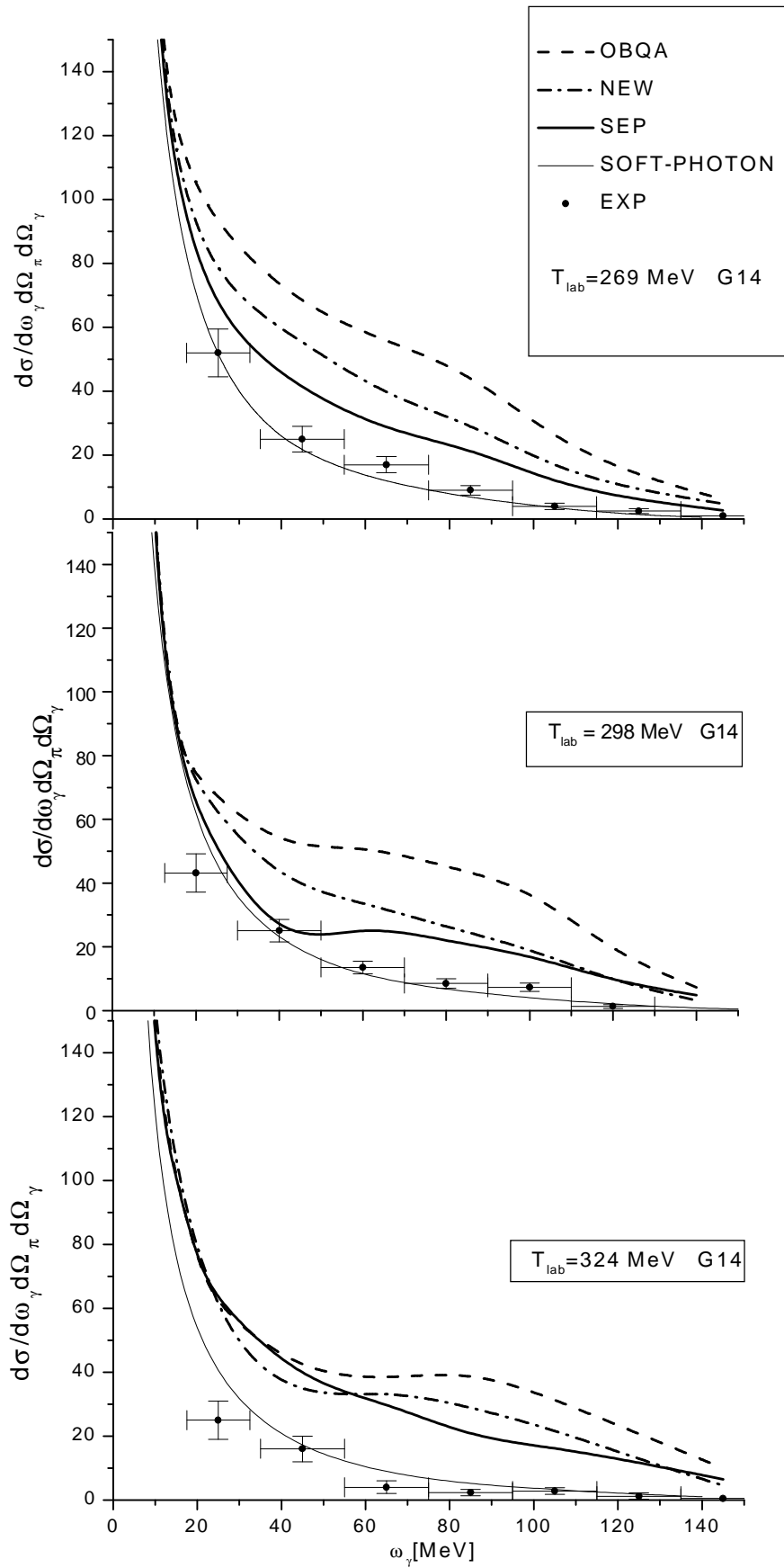


figure 5

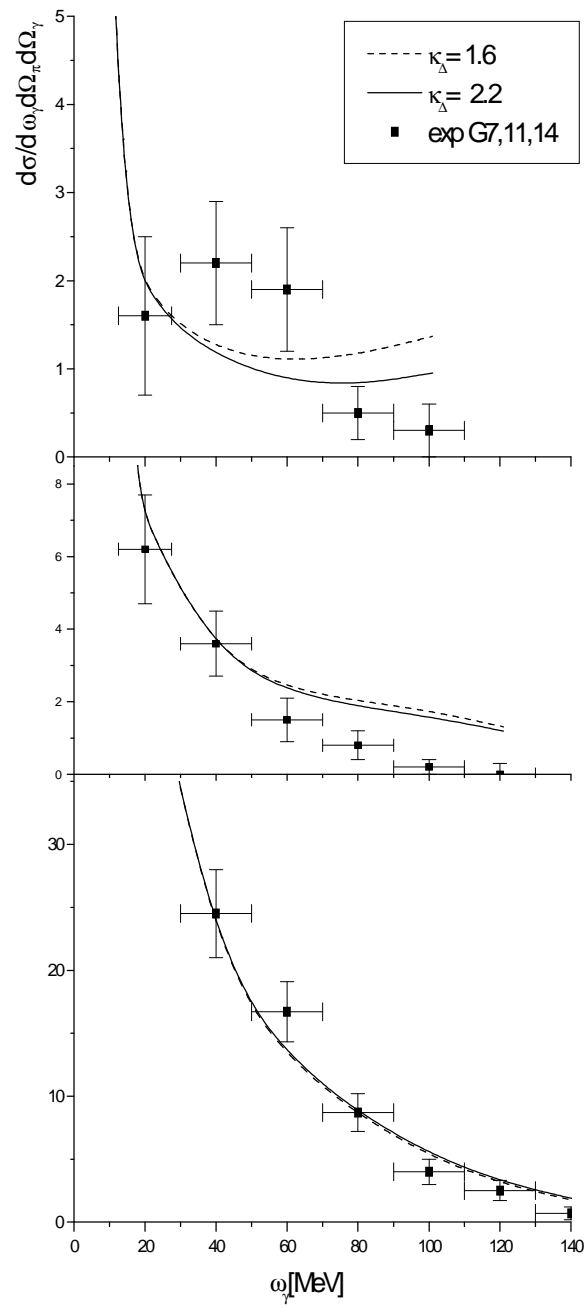


figure6